

Computational Intelligence-Based Fault Detection in Refrigeration Systems: A Study on Enhancing System Reliability

V. Cardoso-Fernández
*Unidad de Posgrado e Investigación,
Facultad de Ingeniería
Universidad Autónoma de Yucatán
Mérida, Yucatán, México*
<https://orcid.org/0000-0002-8554-276X>

Luis J. Ricalde
*Unidad de Posgrado e Investigación,
Facultad de Ingeniería
Universidad Autónoma de Yucatán
Mérida, Yucatán, México*
<https://orcid.org/0000-0001-5824-1454>

A. Bassam
*Unidad de Posgrado e Investigación,
Facultad de Ingeniería
Universidad Autónoma de Yucatán
Mérida, Yucatán, México*
<https://orcid.org/0000-0001-7526-6952>

Abstract—The utilization of computational intelligence, particularly Artificial Neural Networks (ANNs), for fault detection is of paramount importance as it empowers industries to proactively identify anomalies, leading to improved system reliability, reduced downtime, and enhanced safety. By leveraging the pattern recognition capabilities of ANNs, complex data patterns indicative of faults can be accurately identified and analyzed in real-time, enabling early intervention and preventing potential catastrophic failures. Additionally, the importance of fault detection in refrigeration systems lies in its ability to proactively identify and address potential issues, ensuring optimal performance, energy efficiency, and longevity of the system while preventing costly breakdowns and ensuring product safety and quality. The main aim of this study is to create a computational intelligence model that can accurately depict the energy and exergy performance of a GAX hybrid refrigeration system. Moreover, the model aims to identify potential instrument failures occurring at different parts of the system. The primary findings indicate that creating a numerical database using the governing equations of the GAX system enables the identification of anomalies in the instrumental measurements of operating parameters. Subsequent research aims to incorporate experimental data from a broader range of parameters, encompassing additional sections of the GAX system.

Keywords—Artificial neural networks (ANNs), refrigeration systems, fault detection.

I. INTRODUCTION

Computational intelligence has emerged as a powerful technique for detecting failures in various domains, with artificial neural networks (ANNs) playing a crucial role in this endeavor. ANNs are computational models inspired by the human brain's neural structure, capable of learning patterns and relationships from large datasets. Through their ability to process complex and high-dimensional data, ANNs have shown remarkable success in fault detection and diagnosis tasks [1]. Recent research highlights the effectiveness of computational intelligence-driven approaches, especially ANNs, in identifying failures in renewable energy systems, such as wind turbines [2]. These techniques leverage sophisticated algorithms, such as deep learning, to automatically identify anomalies, enabling proactive maintenance and mitigating potentially catastrophic consequences [3]. The adoption of computational intelligence

for failure detection has garnered substantial interest and is expected to further advance various industries, improving reliability and safety while reducing operational costs.

Refrigeration systems powered by renewable energy have gained significant attention in recent years as environmentally friendly alternatives to conventional cooling technologies. One promising approach in this domain is the use of the generator-absorber (GAX) cycle, which has been extensively studied for its potential in improving the efficiency and sustainability of refrigeration systems. The GAX cycle utilizes renewable energy sources, such as solar or geothermal power, to drive the refrigeration process, making it highly attractive for reducing greenhouse gas emissions and minimizing the environmental impact. Considering some of the most representative research done in this area, a solar-powered GAX refrigeration system was proposed and analyzed, demonstrating its feasibility and energy-saving capabilities [4]. Additionally, the performance of a geothermal-powered GAX cycle has also been investigated, highlighting its potential for applications in remote areas with abundant geothermal resources [5]. Such studies signify the growing interest in harnessing renewable energy for refrigeration purposes and emphasize the potential of the GAX cycle as an innovative and sustainable solution for cooling needs.

A key aspect regarding the merging of these two topics lies in the utilization of ANNs to simulate the complex interactions and dynamics of refrigeration systems. ANNs have demonstrated their capability to learn intricate patterns from extensive data, enabling accurate predictions of system behavior under various operating conditions. By using an ANN-based model, it is possible to analyze the energy performance of a refrigeration system, showcasing the potential of computational intelligence-driven approaches in enhancing the system's overall efficiency [6]. Similarly, an ANN model can be used to analyze and improve the mass transfer of a GAX cycle, resulting in enhanced system performance and energy savings [7]. These studies exemplify the increasing adoption of computational intelligence techniques, particularly ANNs, in the field of hybrid refrigeration, offering valuable insights into system behavior and optimization strategies, thereby contributing to more sustainable and environmentally friendly cooling solutions.

The present work uses an ANN model to detect measurement errors at different sections of a GAX hybrid system. The novelty consists in training the computational intelligence technique with a numerical database generated by an exergy analysis of the GAX system, powered by both renewable and non-renewable energy. This document is divided in the following sections: Section II contains the materials and methods, which contains the system description, an exergy analysis, and the computational intelligence technique. Section III presents the results and discussion of the main outcomes.

II. MATERIALS AND METHODS

A. System description

Fig. 1 shows the schematic diagram of the GAX cycle, to describe each stage of the system in detail. The cycle begins at the outlet of the rectifier, where the NH_3 vapor at high system pressure is directed to the condenser, with a purity of 99%. Once inside this element, it is converted to a saturated liquid and sent to the pre-cooler, to reduce its temperature. The fluid passes through a pressure valve (V1), becoming a liquid-vapor mixture at low pressure. Once inside the evaporator, the mixture receives the heat from the water to be cooled, thus generating the cooling effect for the corresponding application. When leaving the evaporator, the mixture passes through the pre-cooler again, which, acting as a heat exchanger, allows the heat coming from the flow in the opposite direction to be used to evaporate the liquid that was still present in the mixture. This cooled vapor now enters the lower part of the absorber, where it is absorbed by the low ammonia NH_3/H_2O solution. Due to the exothermic phase changes that occur, heat exchangers are required in this zone of the absorber. The aqueous solution or strong solution, now with a high percentage of refrigerant, is pumped at high pressure to the next absorber element (AHX), where it receives heat from the absorber. Upon entering the hotter element (GAX), the solution receives even more heat from the absorber, reaching its saturation point as it leaves the column as a liquid-vapor mixture. The mixture enters a chamber located between the generator and rectifier, where the liquid phase from the absorber encounters the condensed vapor from the rectifier. Once inside the generator, the refrigerant is drawn from the solution, turning it into a weak solution and exiting at the bottom of the generator column. The solution is heated in the generator through external heat sources (in this case natural gas and solar thermal energy) and delivers this energy in the GHX section. The second pressure valve (V2) returns it to low pressure, making it possible for it to be reintroduced to the top of the absorber, where it meets the refrigerant vapor. While in the lower part of the generator, the refrigerant vapor rises through the column until it reaches the rectifier, where the heavier elements (H_2O) are condensed. This results in a refrigerant with a high degree of purity, ready to restart the cycle [8]. To replicate this work, the characteristics mentioned in Table 1 should be considered.

Table 1 Main operating conditions of the GAX system.

Mass flow		
<i>System elements</i>	<i>Value</i>	<i>Units</i>
Weak solution	13.302×10^{-3}	kg/s
Strong solution	22.565×10^{-3}	kg/s
Refrigerant	9.263×10^{-3}	kg/s
Cooling air in the absorber	1.306	m ³ /s
Cooling air in the condenser	1.410	m ³ /s
Cooling air in the rectifier	0.270	m ³ /s
Thermal oil	0.122	kg/s
Ammonia concentration		
<i>System elements</i>	<i>Value</i>	<i>Units</i>
Weak solution	3.99	%
Strong solution	43.15	%
Refrigerant	99.39	%
Cold water generation		
<i>System elements</i>	<i>Value</i>	<i>Units</i>
Evaporator inlet temperature	16	°C
Evaporator outlet temperature	10	°C
Mass flow	0.419	kg/s
Pressure		
<i>System elements</i>	<i>Value</i>	<i>Units</i>
Generator	2.0	MPa
Condenser	2.0	MPa
Evaporator	0.5	MPa
Absorber	0.5	MPa

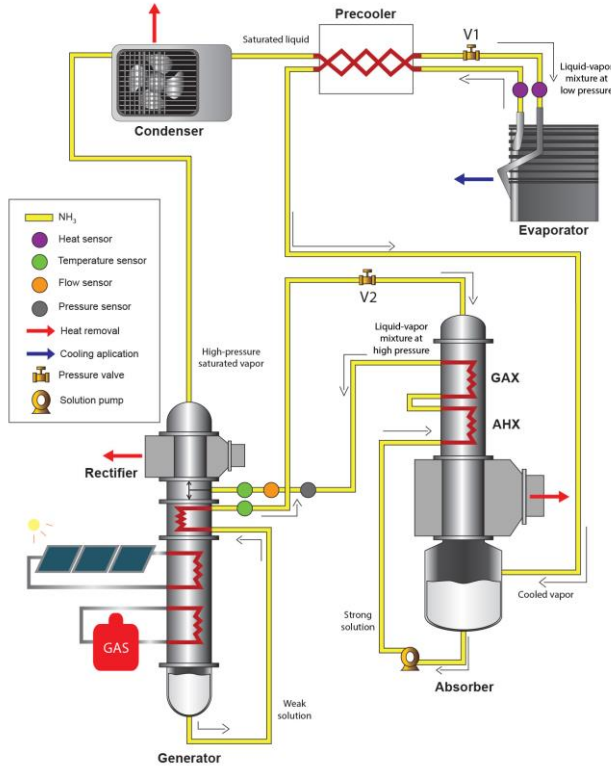


Fig. 1 Schematic diagram of the GAX cycle, consisting of a generating column with coupled rectifier, condenser, precooler, evaporator and the absorber column with GAX and AHX sections.

B. Exergy analysis

To carry out the study of the GAX cycle, it is necessary to establish the equation that governs the exergetic behavior of the system [9], as it is stated in (1):

$$\sum_{i=1}^n \dot{m}_i \dot{e}x_i = \sum_{j=1}^m \dot{m}_j \dot{e}x_j + \text{Irr}_{\text{comp}} \quad (1)$$

Where the index i from 1 to n indicates the n input states, the index j from 1 to m indicates the m output states. Regarding \dot{m} and $\dot{e}x$, these are the mass flows and exergies reported for the states analyzed, while Irr represents the irreversibilities associated with the component studied. By using (1), it is possible to state that the irreversibilities measured for the generator (2), as well as for the overall GAX system (3), are:

$$\text{Irr}_{\text{gen}} = \sum_{j=1}^m \dot{m}_{j,\text{gen}} \dot{e}x_{j,\text{gen}} - \sum_{i=1}^n \dot{m}_{i,\text{gen}} \dot{e}x_{i,\text{gen}} \quad (2)$$

$$\text{Irr}_{\text{gax}} = \sum_{j=1}^m \dot{m}_{j,\text{gax}} \dot{e}x_{j,\text{gax}} - \sum_{i=1}^n \dot{m}_{i,\text{gax}} \dot{e}x_{i,\text{gax}} \quad (3)$$

C. Computational intelligence technique

Due to the ease of synthesizing the operation of complex systems and learning through previously known values, artificial neural networks (ANN) are presented as a powerful solution to the task of processing large amounts of data.

This technique consists of using the independent variables of the problem as input neurons, and the dependent variables as output neurons. These layers of neurons are connected by a hidden layer, whose main purpose is to establish a black-box relation between the known input and the expected output. Additionally, a training algorithm is used, so that the ANN can learn from a database supplied by the user.

To evaluate the performance of the computational intelligence model, three statistical parameters are used. The Pearson correlation coefficient (R) is a statistical metric that quantifies the extent of linear correlation between two variables, and is defined in the following manner:

$$R_{AB} = \frac{\text{cov}(A,B)}{\sigma_A \sigma_B} \quad (4)$$

Where $\text{cov}(A,B)$ is the covariance between the variables A and B , and σ_A, σ_B are the standard deviations of A and B , respectively [10]. The second statistical parameter is the mean absolute percentage error (MAPE), which is calculated by taking the average of every absolute percentage error between real data and the one calculated, as it is stated in the following equation:

$$\text{MAPE} = \frac{1}{N} \sum_{n=1}^N \left| \frac{y_n - t_n}{y_n} \right| \times 100 \quad (5)$$

Where N is the total amount of data, y is the actual value and t the forecast value. The equation is multiplied by 100, to obtain the percentage parameter [11]. The third parameter used is the root mean square error (RMSE), which represents the square root of the average of the squared differences between the predicted and actual values:

$$\text{RMSE} = \sqrt{\frac{1}{N} \sum_{n=1}^N (y_n - t_n)^2} \quad (6)$$

Where N , y , and t represent the parameters mentioned previously in (5) [12].

III. RESULTS AND DISCUSSIONS

A numerical experiment is carried out, to obtain a database capable of representing the thermodynamic relations that takes place in the GAX system. The independent variables considered were the type of solar collector used as thermal supply for the generator, the number of collectors and the mass rate. Additional information regarding the solar technologies is provided in Table 2. As for the dependent variables, they were the mitigated carbon (CCM), net present value (NPV), solar thermal energy (ETH), auxiliary thermal energy (EAUX) and the irreversibilities measured at the generator (IRR_{GEN}) and for the global system (IRR_{GLO}).

Table 2. Design parameters considered for the renewable energy technologies.

Flat plate collector		
Parameter	Value	Units
Length	2.099	m
Width	1	m
Separation of cover and plate	0.254	m
Separation of absorber plate and insulator	0.0254	m
Insulation thickness	0.025	m
Edge thickness	0.019	m
Tilt angle	21	degrees
Parabolic trough collector		
Parameter	Value	Units
Length	5.508	m
Parabola opening width	1.594	m
Receiver tube outer diameter	0.028	m
Receiver tube inner diameter	0.026	m
Edge angle at maximum radius	90	degrees

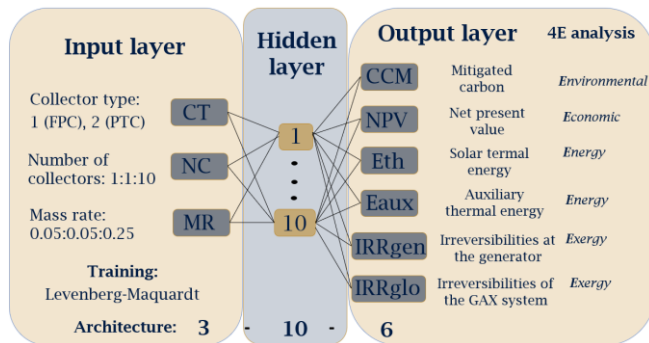


Fig. 2 Schematic representation of the ANN model used for failure detection of the GAX system.

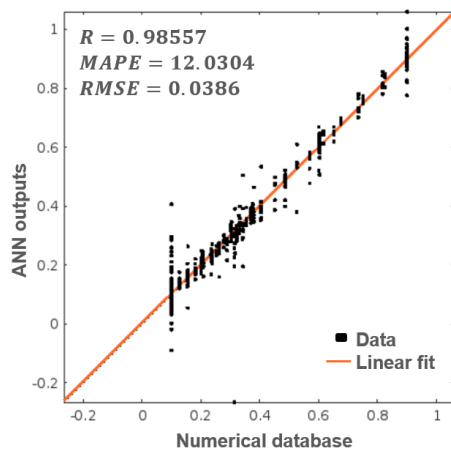


Fig. 3 Performance analysis of the ANN model, considering the six dependent variables of the GAX system.

By using the dataset created from the numerical experiment, a computational intelligence model based on ANN is created. This model generates a black box relation between the input parameters, which are the independent variables considered in the numerical experiment, and the output variables, represented by the dependent variables of the GAX system. The training method used was Levenberg-Maquardt, obtaining an ANN with architecture 3-10-6. Figure 2 is a schematic representation of such ANN model. Additionally to the previous described features, it can be seen that in the input layers, there were different conditions considered for each neuron. For instance, the type of collectors considered for this work where flat plate collector (FPC) and parabolic trough collector (PTC). The model considers a variation of the number of collectors from 1 to 10, with an increment of 1; and a mass rate of 0.05 to 0.25 kg/s, with an increment of 0.05 for each step.

With this configuration, it was possible to create a model with acceptable statistic parameters. As it is shown in Figure 3, the ANN model presents an adequate performance regarding the representation of the GAX system, by achieving a Pearson correlation coefficient of $R = 0.98557$, $MAPE = 12.0304$ and $RMSE = 0.0386$.

Once the computational intelligence model was properly trained, it was used to detect potential measurement errors from the GAX system. As it can be seen in Tables 3 and 4, the mass flow at the generator outlet was modified, from the 0.7901 kg/s which is used normally by the system, to a value of 1.5 kg/s. Such variation led to negative irreversibilities at the generator $IRRGEN = -70.0723$ J and in the GAX system $IRRGLO = -70.2351$ J. The mass flow at the generator outlet was chosen for this numerical experiment, as it is a parameter that depends on the different energy sources that may be coupled to the GAX system.

Table 3. Numerical results of the ANN model with positive irreversibilities.

Operational conditions of the GAX system		
Parameter	Value	Units
Mass flow at generator outlet	0.7901	kg/s
Outputs obtained by the ANN model		
Parameter	Value	Units
Mitigated carbon (CCM)	56.8562	kg CO ₂
Net present value (NPV)	87,291	\$ USD
Solar thermal energy (ETH)	88,373	kWh
Auxiliary thermal energy (EAUX)	2,595.6	kWh
Irreversibilities at the generator (IRRGEN)	25.5429	J
Irreversibilities of the system (IRRGLO)	25.5422	J

Table 4. Numerical results of the ANN model with negative irreversibilities.

Operational conditions of the GAX system		
Parameter	Value	Units
Mass flow at generator outlet	1.5	kg/s
Outputs obtained by the ANN model		
Parameter	Value	Units
Mitigated carbon (CCM)	57.8273	kg CO ₂
Net present value (NPV)	84,670	\$ USD
Solar thermal energy (ETH)	90,580	kWh
Auxiliary thermal energy (EAUX)	2,666.6	kWh
Irreversibilities at the generator (IRRGEN)	-70.0723	J
Irreversibilities of the system (IRRGLO)	-70.2351	J

If an error like the negative irreversibilities shown in Table 4 arises, the ANN model will be capable of detecting it and sending a message to the user. Such action is activated by using a string type block, created with conditional clauses which identifies when an experimental measured variable does not agree with the theoretical expected value. As it is not possible to obtain negative irreversibilities, the messages displayed by the computational intelligence model are:

Fault detection (IRRGEN): A negative irreversibility was detected at the generator. Please check the instruments used to measure mass flow, temperature, and pressure at the generator, as this error is due to a malfunction in the measuring instruments.

Fault detection (IRRGLO): A negative irreversibility was detected at the GAX system. Please check the instruments used to measure mass flow, temperature, and pressure at the generator, absorber, condenser, and evaporator, as this error is due to a malfunction in the measuring instruments.

As explained before, the energy source used at the generator is a major element of disruption, as different solar technologies may affect the operating parameters measured at this section. For future research, it is intended to expand the database used to train the computational intelligence model, by considering a wide range of energy sources, both renewable and nonrenewable. Furthermore, additional measurement instruments may be added at different sections of the GAX cycle, to detect errors in different parts of the system. Additional aspects of this study could encompass identifying various other failures, including an inaccurate coefficient of performance (COP) caused by measurement errors in mass flow, working fluid temperature, or pressure at different parts of the GAX system. As more variables are targeted for measurement, it might be necessary to utilize a distinct training algorithm or even consider a different computational intelligence technique. All these fault detection

instruments would contribute to a decision-making process, wherein the replacement of a mass flow sensor, pressure sensor, or temperature sensor might occur within a specific section of the refrigeration system.

ACKNOWLEDGMENT

The author V. Cardoso-Fernández is grateful for the financial support of CONAHCYT (*Consejo Nacional de Humanidades, Ciencias y Tecnologías*), to pursue a postgraduate degree in *Facultad de Ingeniería, Universidad Autónoma de Yucatán*, under the following details: CVU: 1006703 and scholarship number: 752330.

REFERENCES

- [1] S. Heo and J. H. Lee, "Fault detection and classification using artificial neural networks," *IFAC-PapersOnLine*, vol. 51, no. 18, pp. 470–475, 2018, doi: 10.1016/j.ifacol.2018.09.380.
- [2] G. Helbing and M. Ritter, "Deep Learning for fault detection in wind turbines," *Renew. Sustain. Energy Rev.*, vol. 98, pp. 189–198, Dec. 2018, doi: 10.1016/j.rser.2018.09.012.
- [3] L. W. Alabe, K. Kea, Y. Han, Y. J. Min, and T. Kim, "A Deep Learning Approach to Detect Anomalies in an Electric Power Steering System," *Sensors*, vol. 22, no. 22, p. 8981, Nov. 2022, doi: 10.3390/s22228981.
- [4] S. Q. Abu-Ein, S. M. Fayyad, W. Momani, and M. Al-Bousoul, "Performance analysis of solar powered absorption refrigeration system," *Heat Mass Transf.*, vol. 46, no. 2, pp. 137–145, Dec. 2009, doi: 10.1007/s00231-009-0538-1.
- [5] F. Musharavati, S. Khanmohammadi, and R. Tariq, "Comparative exergy, multi-objective optimization, and extended environmental assessment of geothermal combined power and refrigeration systems," *Process Saf. Environ. Prot.*, vol. 156, pp. 438–456, Dec. 2021, doi: 10.1016/j.psep.2021.10.018.
- [6] J. M. Belman-Flores and S. Ledesma, "Statistical analysis of the energy performance of a refrigeration system working with R1234yf using artificial neural networks," *Appl. Therm. Eng.*, vol. 82, pp. 8–17, May 2015, doi: 10.1016/j.applthermaleng.2015.02.061.
- [7] O. May Tzuc et al., "Multivariate inverse artificial neural network to analyze and improve the mass transfer of ammonia in a Plate Heat Exchanger-Type Absorber with NH₃/H₂O for solar cooling applications," *Energy Explor. Exploit.*, p. 014459872110731, Feb. 2022, doi: 10.1177/01445987211073175.
- [8] M. A. Barrera, R. Best, V. H. Gómez, O. García-Valladares, N. Velázquez, and J. Chan, "Analysis of the performance of a GAX hybrid (Solar - LPG) absorption refrigeration system operating with temperatures from solar heating sources," *Energy Procedia*, vol. 30, pp. 884–892, 2012, doi: 10.1016/j.egypro.2012.11.100.
- [9] D. Colorado, N. Demesa, A. Huicochea, and J. A. Hernández, "Irreversibility analysis of the absorption heat transformer coupled to a single effect evaporation process," *Appl. Therm. Eng.*, vol. 92, pp. 71–80, Jan. 2016, doi: 10.1016/j.applthermaleng.2015.09.076.
- [10] V. A. Profillidis and G. N. Botzoris, "Statistical Methods for Transport Demand Modeling," in *Modeling of Transport Demand*, Elsevier, 2019, pp. 163–224. doi: 10.1016/B978-0-12-811513-8.00005-4.
- [11] S. Kim and H. Kim, "A new metric of absolute percentage error for intermittent demand forecasts," *Int. J. Forecast.*, vol. 32, no. 3, pp. 669–679, Jul. 2016, doi: 10.1016/j.ijforecast.2015.12.003.
- [12] P. Singla, M. Duhan, and S. Saroha, "Different normalization techniques as data preprocessing for one step ahead forecasting of solar global horizontal irradiance," in *Artificial Intelligence for Renewable Energy Systems*, Elsevier, 2022, pp. 209–230. doi: 10.1016/B978-0-323-90396-7.00004-3.